PRE-ALLEGHANIAN EXTENSION AND POST-ALLEGHANIAN BRITTLE DEFORMATION IN THE SOUTHERN APPALACHIANS

Sarah Brook Wells-Hull

A thesis submitted to the faculty at the University of North Carolina at Chapel Hill in partial fulfillment of the requirements for the degree of Master of Science in the Department of Geological Sciences.

Chapel Hill
2022

Approved by:

Kevin Stewart

Jonathan Lees

Tamlin Pavelsky

ABSTRACT

Sarah Brook Wells-Hull: Pre-Alleghanian extension and post-Alleghanian brittle deformation in the southern Appalachians
(Under the direction of Kevin G. Stewart)

Thrust faults related to the orogenic events that formed the Appalachians dominate the Blue Ridge province in western North Carolina, but no clear extensional faults have been identified. We discovered the first documented pre-Alleghanian normal fault within the southern Appalachian Blue Ridge, the Grassy Creek fault (GCf). The GCf may be associated with synorogenic or pre-collisional extension and may also explain the exhumation of an eclogite facies terrane within the Ashe Metamorphic Suite.

A set of topographic lineaments in western North Carolina cut the Paleozoic structures and do not correspond with the well-documented geologic history of the southern Appalachians. One of these lineaments corresponds to the Boone fault, which likely accommodates Miocene uplift of the southern Appalachians. We performed fracture and paleostress analyses along lineaments north of the Boone fault, which indicate that they are likely fracture controlled and related to the same deformation event responsible for the Boone fault.

ACKNOWLEDGMENTS

I would like to thank my advisor, Kevin Stewart, for his guidance throughout this process and his encouragement through all of our findings. Thanks to my committee members, Jonathan Lees and Tamlin Pavelsky. This project was made possible through funding from the EDMAP Award G20AC00132, the Geological Society of America student research grant, and the Martin Annual Research Fund awarded through the UNC Department of Geological Sciences. Thank you to Richard Wooten, Jesse Hill, and Bart Cattanach from the North Carolina Geological Survey for their time in the field. Special thanks to my field assistant, Sage Turek, for her hard work and positivity during mapping. I would also like to thank the residents of Watauga County for access to their land and their kindness and interest in this work. I would like to thank my friends and family, especially my husband, Travis Hull, for the endless support and prayers throughout this process.

TABLE OF CONTENTS

LIST OF FIGURES

Introduction

Normal faults and extensional fabrics in collisional mountain chains are often thought to result from orogenic collapse that follows mountain building (Dewey, 1988). However, synorogenic and pre-collisional normal faults have been identified within the Himalayas (England and Houseman, 1989), the Alps (Behrmann, 1988; Avigad, 1996), and the Andes (Dalmayrac and Molnar, 1981). Synorogenic normal faults have been attributed to internal extension due to buoyancy forces (Searle and Lamont, 2020) or underplating and overthickening of the crust (Platt, 1986). Pre-collisional normal faults may form as a result of subduction creating extension prior to terrane accretion (Gun et al., 2021). Synorogenic and pre-collisional extension have been proposed as a method for exhuming high-pressure metamorphic rocks, such as eclogites, and juxtaposing them at structurally higher levels with lower-pressure metamorphic rocks (Platt, 1986; Behrmann, 1988; Avigad, 1996; Adlakha et al., 2013; Searle and Lamont, 2020; Gun et al., 2021).

The southern Appalachian Blue Ridge province is dominated by thrust faults that formed when island arcs, microcontinents, and Gondwana accreted onto the eastern margin of Laurentia (Hatcher et al., 2005; Hatcher et al., 2010), but little evidence for extension has been identified. Apart from the evidence of late Precambrian extension along the Fries fault (Simpson and Kalaghan, 1989), no clear extensional faults have been identified within the southern Appalachian Blue Ridge. However, we discovered an amphibolite facies normal fault within the Eastern Blue Ridge that corresponds to the previously mapped lithologic contact between the

Ashe and Alligator Back Metamorphic Suites (Figure 1). At amphibolite facies metamorphism, the Grassy Creek fault is likely pre-Alleghanian and one of the first amphibolite facies normal faults identified in the southern Appalachians.

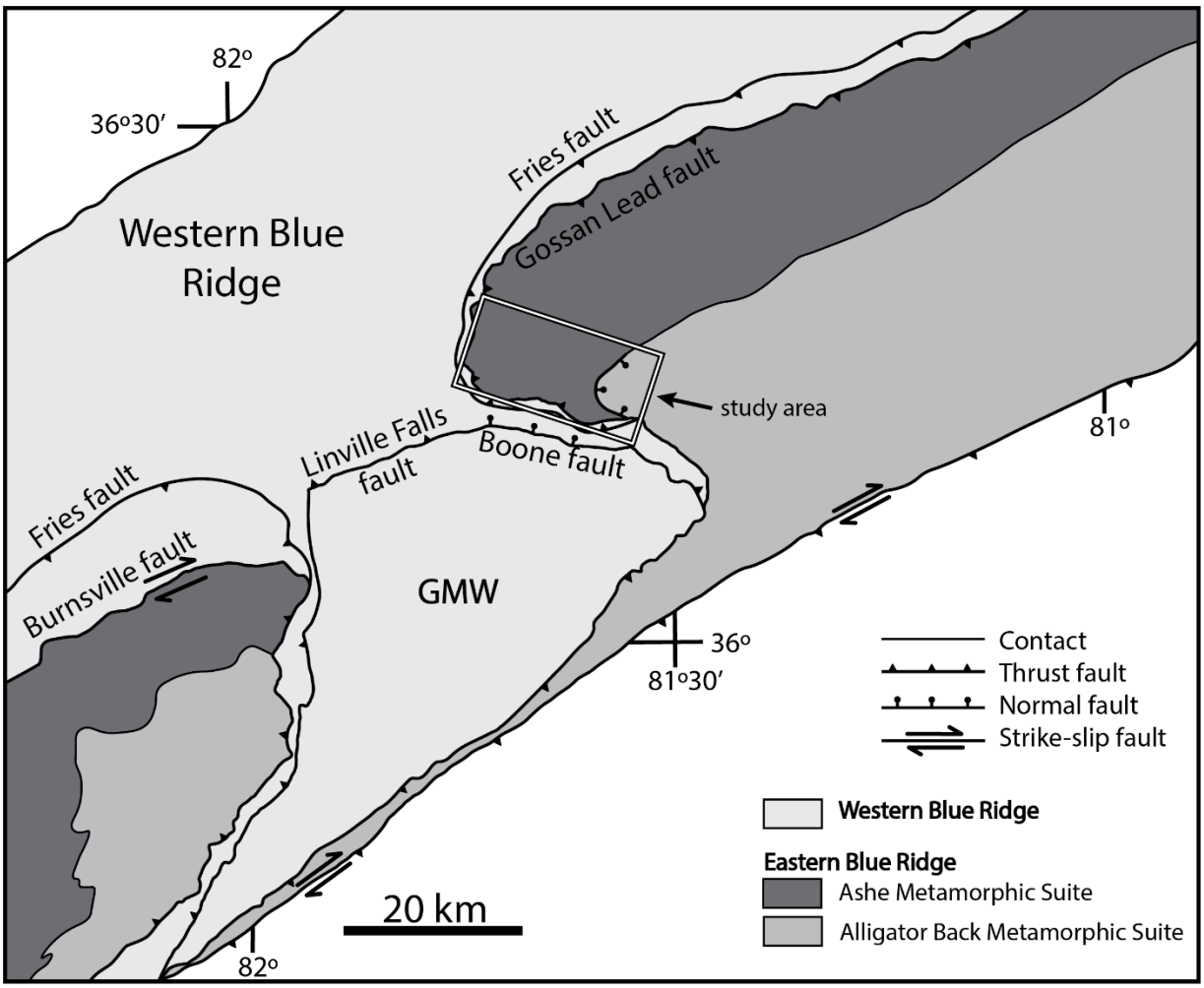

Figure 1: Simplified map of the Eastern and Western Blue Ridge in western North Carolina. Inset box shows location of study area. Modified from Hatcher et al. (2006).

In addition to the ductile normal fault, this area is also characterized by topographic lineaments that cut the topography of the southern Appalachians and post-date the synorogenic deformation of the southern Appalachians (Figure 2). Despite the lack of an active plate boundary since the late Triassic, the Appalachians share characteristics with tectonically active

settings. For example, sediment accumulation in the Atlantic and the Gulf of Mexico increased abruptly during the Middle Miocene (Galloway et al., 2011), which Poag and Sevon (1989) interpreted to be the result of tectonic uplift, weathering, and rapid erosion of the Appalachians. Similarly, Dennison and Stewart (2001) proposed that the sudden influx of coarse clastics into the coastal plain in the early Miocene resulted from uplift of the southern Appalachian Blue Ridge. Dennison and Stewart (2001) also speculated that topographic lineaments that cut the Paleozoic topography were fracture zones that formed in response to the uplift. The topographic lineaments, corresponding to linear valleys, appear to be related to recent uplift of the southern Appalachians.

Recently, Hill (2018) found that one of these lineaments near Boone, NC, corresponds to a Neogene high angle dip-slip fault named the Boone fault (Figure 2). Hill (2018) proposed that vertical movement along the lineaments accommodates blocky uplift resulting from lithosphere delamination beneath the southern Appalachians. Approximately 50 km north of the Boone fault in Sparta, NC, the Little River fault, an active reverse fault that slipped in August 2020, corresponds to a faint topographic lineament (Figure 2; Hill et al., 2020b). Just north of the Boone fault, in Watauga County, NC, a set of lineaments are parallel to the Boone fault (Figure 2). Structural analyses of these lineaments show that they are likely fracture controlled and related to the same deformation event responsible for the Boone fault.

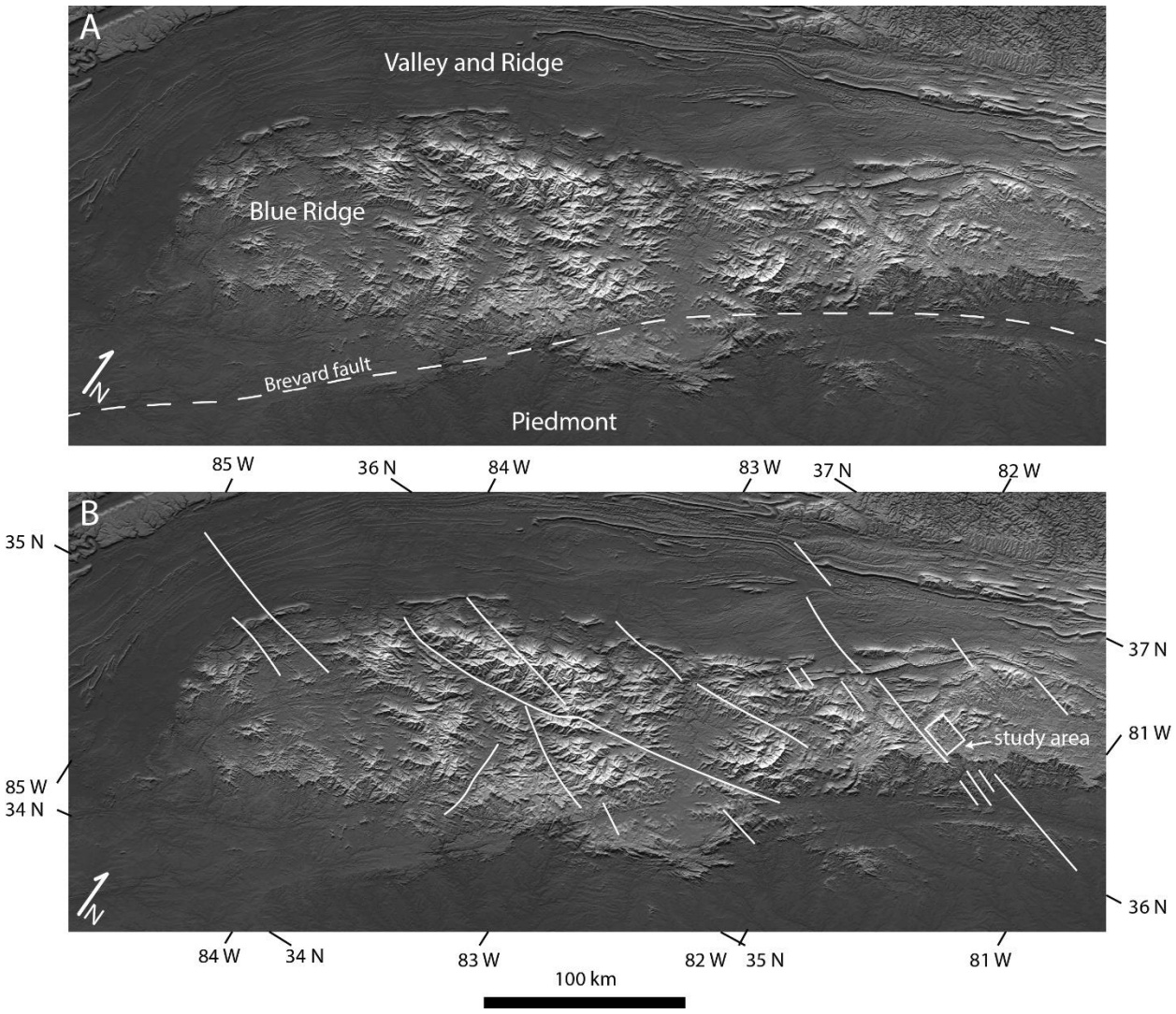

Figure 2: A.) Digital elevation model of the southern Appalachians in North Carolina with major geologic provinces labeled. B.) Topographic lineaments cut the Blue Ridge and Piedmont topography (Hack, 1982; Dennison and Stewart, 2001).

Geological and regional setting

Orogenic events

The Appalachians formed in a complete Wilson cycle that began ~1.2 Ga with the assembly of Rodinia, which produced the Grenville orogeny (Hatcher et al., 2005; Hatcher et al., 2010). The Grenville orogeny was followed by a period of tectonic inactivity, which was interrupted by Neoproterozoic-to-early Paleozoic rifting of Rodinia. Unsuccessful rifting ~735

Ma was followed by successful rifting ~565 Ma, resulting in the opening of the Iapetus Ocean and the deposition of sedimentary rocks that would later become the metasedimentary rocks of the Grandfather Mountain window (GMW) in the southern Appalachians (Figure 1; Hatcher et al., 2007; Tull et al., 2010). After the breakup of Rodinia, three separate orogenies resulted in the formation of the supercontinent Pangea and the Appalachian Mountain range.

The Ordovician Taconic orogeny (~460-455 Ma) formed during the closing of the Iapetus Ocean as the Piedmont terrane collided with Laurentia (Hatcher et al., 2010). Prior to the Taconic orogeny, east-dipping subduction beneath the Piedmont arc system reached eclogite facies conditions at depths of >50 km (Miller et al., 2006). During the Taconic orogeny, thrust faulting brought rocks of the Eastern Blue Ridge (EBR) over the Laurentian basement rocks of the Western Blue Ridge (WBR; Abbott and Raymond, 1984). Rocks in the EBR experienced widespread amphibolite to granulite facies, metamorphism (Abbott and Raymond, 1984).

The Devonian-Mississippian Acadian-Neoacadian orogeny (~410-345 Ma) involved transpressional tectonic as the Rheic ocean closed and Peri-Gondwanan superterranes collided with Laurentia (Hatcher et al., 2010). The record of the Acadian orogeny is well preserved in the northern Appalachians but not as clear in the southern Appalachians. North and south of the GMW, the EBR and WBR are separated by the Gossan Lead and Burnsville faults (Figure 1; Stose and Stose, 1957; Adams et al., 1995). Devonian-Mississippian, amphibolite facies, strike-slip faulting along the Gossan Lead and Burnsville faults structurally cut the Taconic suture between the EBR and the WBR (Trupe et al., 2003; Levine et al., 2018).

The Pennsylvanian-Permian Alleghanian orogeny (~325-265 Ma) resulted from the continent-continent collision that formed supercontinent Pangea, which is widely thought to be responsible for the crustal thickening and topography seen in the southern Appalachians today.

The Blue Ridge experienced greenschist facies conditions as thrusting along the Linville Falls, and Fries faults (Figure 1) transported the Blue Ridge thrust sheet westward (Rankin, 1969; Bryant and Reed, 1970; Hatcher, 2002). North of GMW, thrusting along the Fries fault overprinted the Acadian strike-slip faulting along the Gossan Lead fault (Levine et al., 2018). Mesozoic E-W rifting followed during the break of Pangea.

Ashe and Alligator Back Metamorphic Suites

The Ashe Metamorphic Suite (AMS) and the Alligator Back Metamorphic Suite (ABMS) are the two principal components of the EBR. The ABMS was originally mapped as AMS (Rankin, 1970) but later separated by a non-faulted, lithologic contact based on the distinguishing feature of 'pin-stripe' gneiss (Rankin et al., 1973). In southern Virginia, the AMS and ABMS contact corresponds to the Rock Castle Creek fault, a NW-directed mylonitic fault zone (Carter and Merschat, 2014). South of GMW, Cattanach et al. (2016) also mapped a thrust fault along the AMS and ABMS contact.

The AMS and ABMS were likely once a part of an accretionary wedge complex formed during the subduction of the oceanic lithosphere between the Laurentian craton and the Piedmont terrane (Abbott, 1984; Abbott and Raymond, 1997; Abbott and Greenwood, 2001; Miller et al., 2006). Rocks that dominate the AMS are amphibolite, gneiss, schist, ultramafic rocks, pegmatite, eclogite, and retrograded eclogite. Rocks that dominant the ABMS are gneiss and schist, with small amounts of amphibolite. Rocks within the AMS and ABMS experienced peak metamorphism at amphibolite facies during the Ordovician Taconic orogeny, which is responsible for the well-developed foliation seen in the EBR today. Alleghanian doming of the GMW folded the rocks of the AMS and ABMS north of the GMW to the northeast (Bryant and Reed, 1970; Boyer and Elliot, 1982).

Eclogite in the southern Appalachians was first discovered by Willard and Adams (1994) within the AMS south of the GMW. Along the base of the AMS, north of the GMW, Abbott and Greenwood (2001) identified retrograded eclogite, in the form of amphibolite, distinguished by the amphibolite + feldspar 'coronas' surrounding the garnets. The coronas formed due to a retrograde reaction between the garnet and the surrounding symplectite (Abbott and Greenwood, 2001). The mineralogy and textures indicate amphibolite facies retrogression of an original eclogite assemblage.

Topographic lineaments

A family of lineaments in the southern Appalachians, some of which were recognized by Hack (1982) and others by Stewart and Dennison (2006), have become more apparent after the recent release of LiDAR-based DEMs that now cover the state of North Carolina. These lineaments cut the Valley and Ridge, Blue Ridge, and Piedmont topography, as well as the Brevard fault and other major structures (Figure 2). These features have been described as fault or fracture zones that were likely produced during regional Miocene uplift of the southern Appalachians (Hack, 1982; Stewart and Dennison, 2006; Hill, 2013). Hill (2018) suggests the regional uplift is the result of lithosphere delamination beneath the southern Appalachians and estimates 450-750 m of uplift.

There have been four known earthquakes with a magnitude of five or greater in North Carolina. Each of these four earthquakes appears to correspond to well-defined lineament swarms that trend roughly ESE and E-W (Stewart et al., 2020). One of these earthquakes occurred on August 9th, 2020, with a magnitude of 5.1 in Sparta, North Carolina, producing a surface rupture of the reverse fault responsible for the earthquake. This reverse fault was named the Little River fault (Hill et al., 2020b) and strikes approximately 110˚, which corresponds to

faint topographic lineaments in that area. South of the Little River fault, in Boone, North Carolina, Hill (2018) discovered that a prominent topographic lineament corresponds to a Neogene, high-angle, dip-slip fault that strikes approximately 105˚, known as the Boone fault, and suggests that this feature is attributed to late Cenozoic topographic rejuvenation. Just north of the Boone fault, a set of topographic lineaments are parallel to the Boone fault and appear to be related to the same deformation event responsible for the Boone fault.

Fracture analyses

We mapped bedrock contacts and measured fracture orientations to determine if the lineaments north of the Boone fault correspond with faults or are fracture controlled. The contact between gneiss and amphibolite were mapped across the lineaments in multiple locations and did not show measurable offset (Figure 3). We measured 1,262 fractures throughout the field area. We separated fractures measured within a ~200-meter width around the lineaments to compare to the fractures measured outside of the lineaments. There are 91 fracture measurements from within the lineaments in our field area, 60 within the southernmost lineament (Figure 4; L1), and 31 within the lineament just north of L1 (Figure 4; L2). A lack of data within the remaining lineaments limited our focus to the two southernmost lineaments. We used data for the two lineaments from the western, high topography side of the map where the data could be constrained within the well-defined lineaments. We also compared fractures within the east and west domain, separated from higher to lower topography (Figure 4).

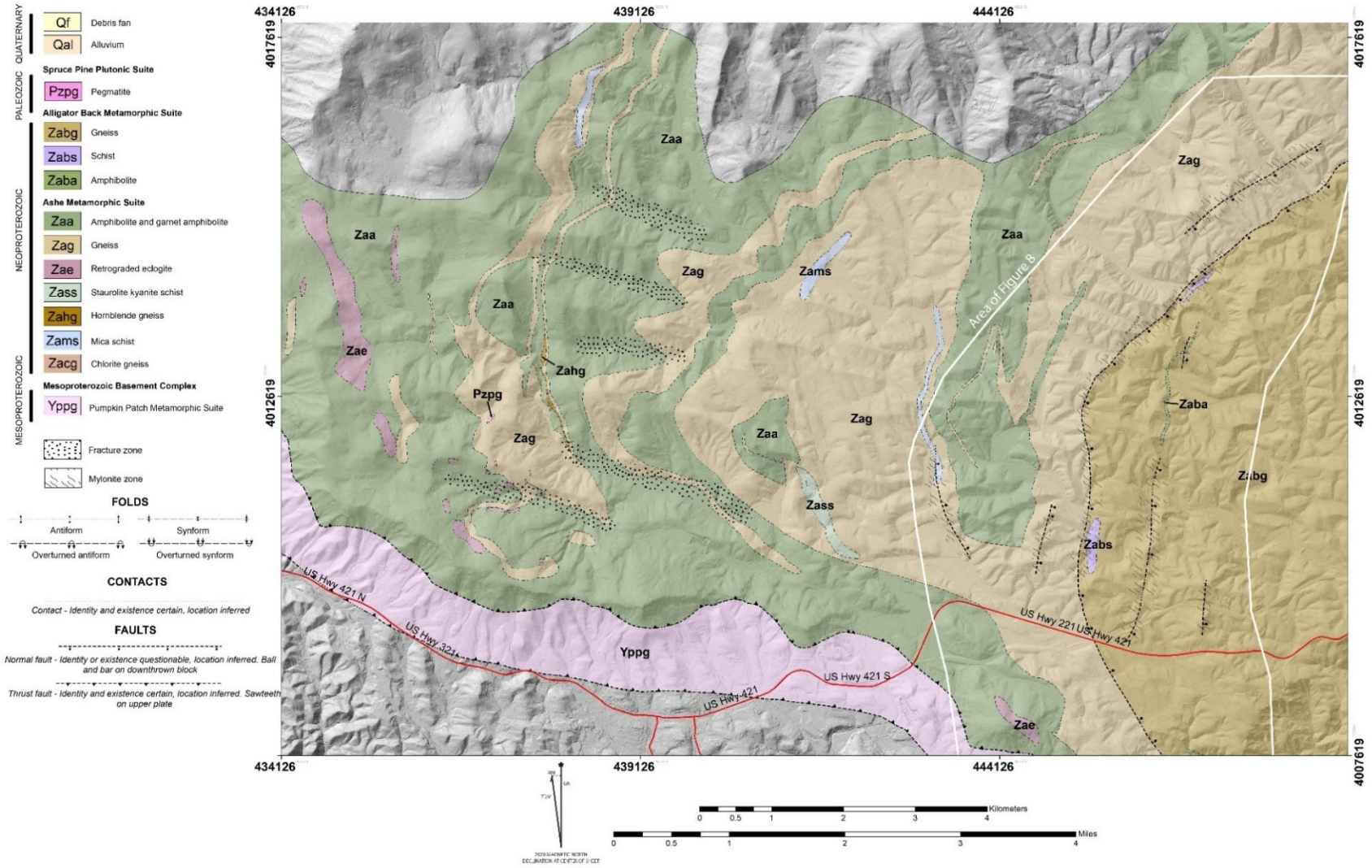

Figure 3: Simplified geologic map of field area. White outline shows the location of Figure 8

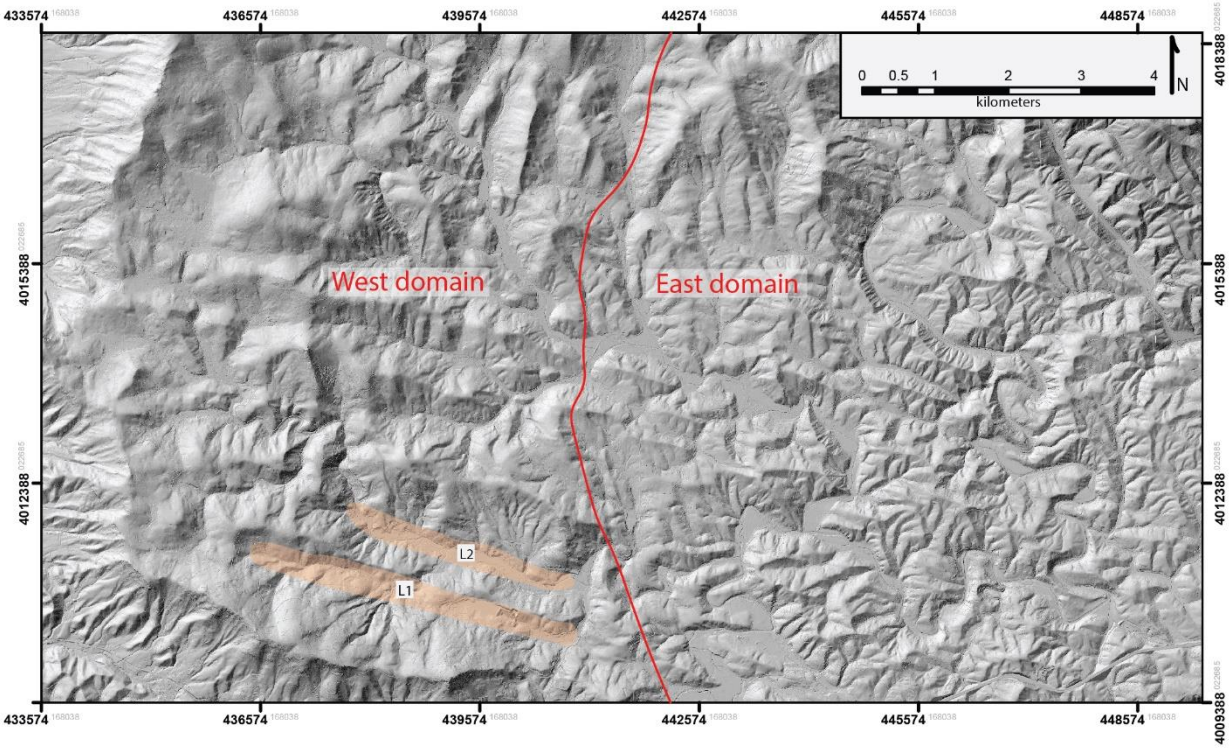

Figure 4: Digital elevation model of map area showing lineaments L1 and L2 highlighted in orange. West domain is characterized by higher topography. East domain is characterized by lower topography.

Equal-area plots show a dominant strike of 108˚ for fractures in L1 (Figure 5a) and 73˚ for L2 (Figure 5b). Fractures outside the lineaments (L0; Figure 5c) also show a dominant E-W striking set as well as NE-SW and NW-SE striking sets. West-domain fractures contain dominant 36˚ and 82˚ striking sets along with NE-SW and NW-SE sets (Figure 5d). East-domain fractures have a dominant strike of 100˚ (Figure 5e). A plot of all fractures shows that the dominant fractures strike 98˚ and 113˚ (Figure 5f). The average trend of the lineaments is 110˚.

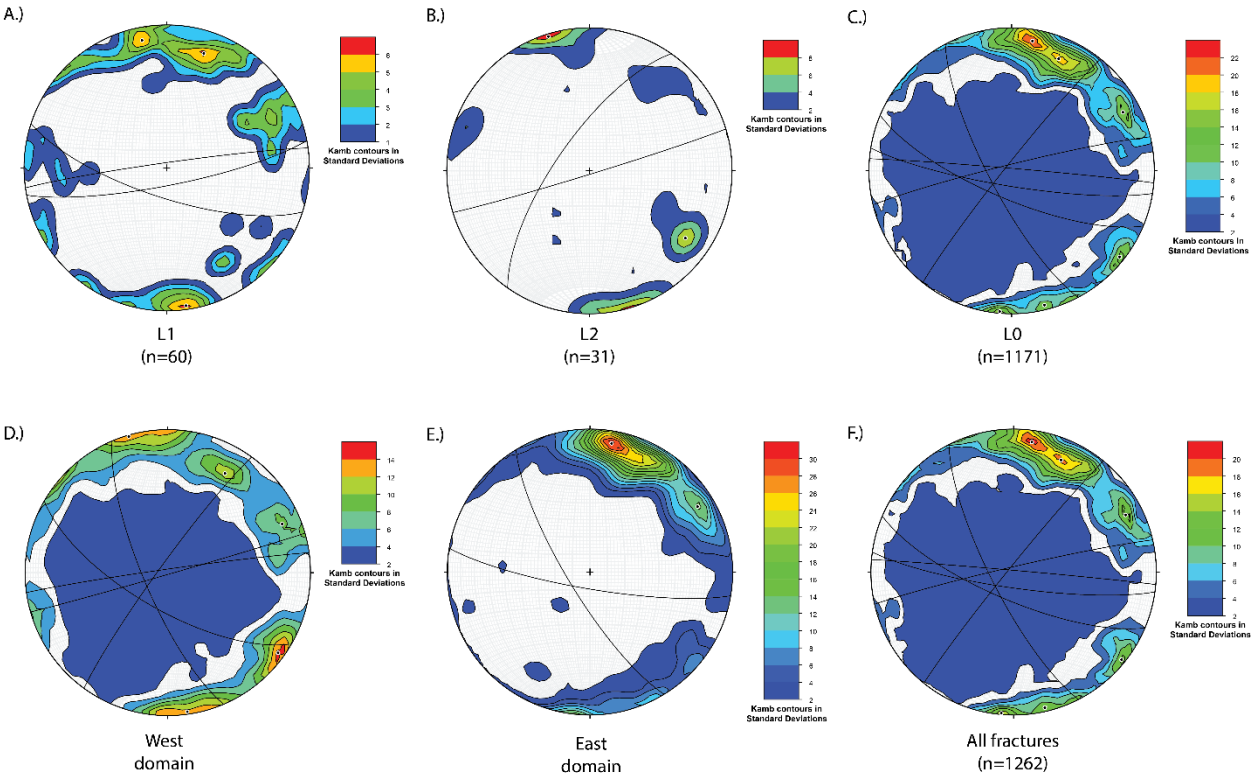

Figure 5: Equal-area plot (lower hemisphere) of contoured poles to fractures and dominant fracture planes represented by great circles. (A) L1 = Lineament 1. Dominant fracture is striking 108 ˚. (B) L2 = Lineament 2. Dominant fracture is striking 73˚. (C) L0 = Lineament 0. Dominant fracture sets strike E-W, SE-NW, and NE-SW. (D) West domain fractures. (E) East domain fractures. Dominant fracture is striking 100˚. (F) All fractures within field area. Dominant fractures are striking 98˚ and 113˚.

Paleostress analyses

We measured faults with slickenlines for paleostress inversion, using the WinTensor program (Delvaux and Sperner, 2003), to estimate the principal stress directions at the time of fault movement. The slip direction on a fault is assumed to be parallel to the maximum shear stress direction on the fault plane. Principal stress tensors describe only the normal stresses and no shear stresses during faulting and can simplify the description of stresses that drive faulting. This gives us information on the stress directions and the timing of brittle deformation within our

map area. Paleostress analyses help constrain the timing of the movement along the faults by comparing the calculated stress tensors to estimated stress directions for previous tectonic events. Examples of Paleozoic NW-directed shortening structures exist throughout the Blue Ridge and should be reflected as a NW-directed maximum compressive stress (Hibbard et al., 2006). Mesozoic rifting should be shown with a vertical maximum compressive stress and east-west-directed minimum compressive stress. Lineaments accommodating NE-SW extension associated with Miocene doming should be reflected by a steep maximum compressive stress and a NE-SW-directed minimum compressive stress (Hill, 2018).

We measured 76 brittle fault surfaces, 42 of which contained slickenlines and were used to perform paleostress inversions. Of those 42 fault surfaces, we separated 27 into two dominant sets of stress tensors. Set A yielded a stress tensor with vertical maximum compression and NE-directed minimum compression and contained nine fault surfaces (Figure 6a). The trend and plunge of the principal stresses for set A are: σ_1 = 028/16; σ_2 = 120/07, σ_3 = 234/72. The engineering naming convention of principal stresses is used, where σ_3 is the greatest compressive stress, and σ_1 is the least compressive stress. Set B yielded a stress tensor with NW-directed maximum compression and contained 18 fault surfaces (Figure 6b). The trend and plunge of the principal stresses for set B are: σ_1 = 076/44; σ_2 = 208/35; σ_3 = 318/26.

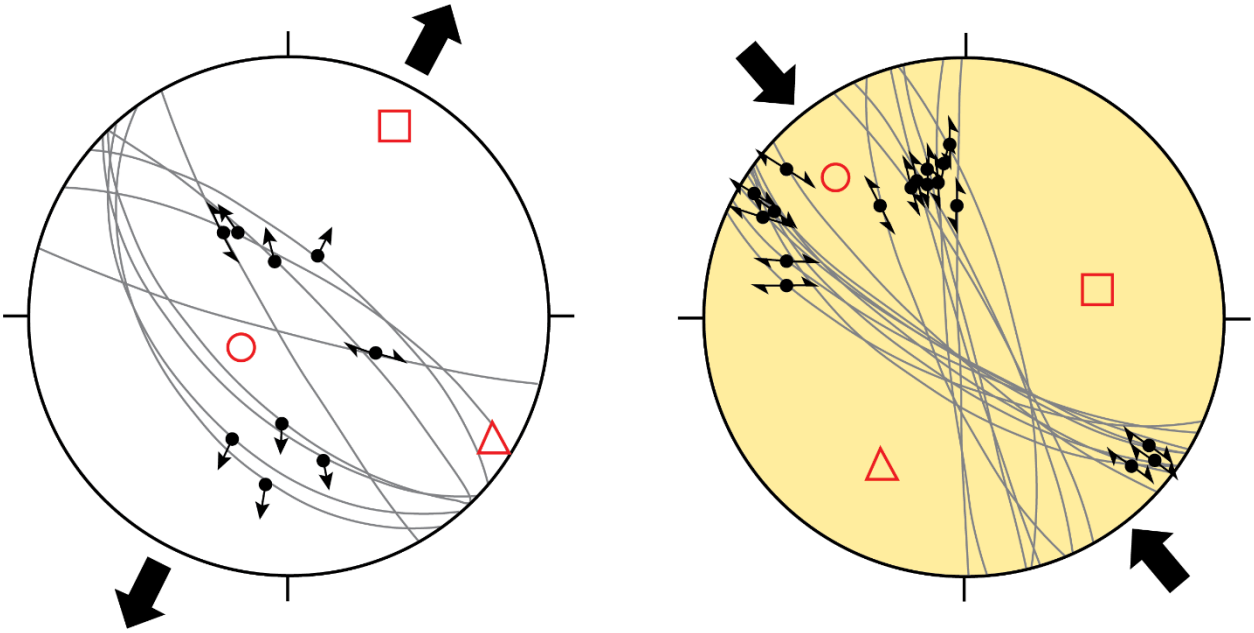

Figure 6: Equal-area, lower-hemisphere plots showing brittle faults (gray lines) with slickenlines (black dots). The paleostress inversions yielded the best fit maximum, intermediate, and minimum compressive stress directions that formed the faults. We are using engineering convention, where σ3 = maximum compression and σ1 = minimum compression. (A) Set A yielding a stress tensor with vertical directed maximum compression and NE directed minimum compression. (B) Set B yielding a stress tensor with NW directed maximum compression.

Ductile normal fault

Synorogenic and pre-collisional normal faults have been identified in multiple actively converging mountain ranges (Platt, 1986; Behrmann, 1988; Avigad, 1996; Adlakha et al., 2013; Searle and Lamont, 2020; Gun et al., 2021). Synorogenic normal faults have been attributed to internal extension possibly due to buoyancy forces or overthickening of the crust (Platt, 1986; Searle and Lamont, 2020). Pre-collisional normal faults have been attributed to extension as a result of the pull of the subducting plate (Avigad, 1996; Gun et al., 2021). Synorogenic and pre-collisional faults are capable of exhuming high-pressure metamorphic rocks, such as eclogite (Platt, 1986; Avigad, 1996).

Thrust faults related to the orogenic events that formed the Appalachian Mountain range dominate the southern Appalachian Blue Ridge province, but no clear extensional faults have been identified. Simpson and Kalaghan (1989) suggest that Alleghanian thrusting along sections of the Fries fault crosscut earlier greenschist facies dip-slip normal fabric associated with late Precambrian extension. We discovered an unmapped ductile normal fault, the Grassy Creek fault, identified by the presence of mylonite (Figure 7).

Figure 7: Mylonitic Alligator Back gneiss (Zabg) contains S-C fabric that indicates top-down-to-SE shear sense (36.239287˚N, 81.607970˚W).

Shear sense determination

Fabric elements and structures in mylonitic rocks show monoclinic symmetry as a result of non-coaxial progressive deformation due to relative displacement of the wall rocks (Passchier and Trouw, 2005). The direction of movement in a shear zone lies subparallel to the mineral-stretching lineations in the rock. In many locations where lineations were present, field determination of shear sense could be made from the S-C fabric visible in outcrop. At these locations, we measured the orientation of the mineral-stretching lineations and noted the shear sense (Figure 8). Mylonitic rocks within the shear zone show a moderate-to-shallow ESE dipping foliation and contain mineral-stretching lineations with an average trend of 158˚and a plunge of 27˚(Figure 8). All shear-sense indicators in outcrop show top-to-SSE motion.

We also collected oriented samples for microstructural kinematic analyses. We determined shear sense in 18 oriented thin sections within the shear zone. Samples that contained observable shear-sense indicators were in the gneiss and schist of the AMS and the ABMS. All thin section shear-sense indicators, including S-C and C' fabric (Figure 9a, b) and rotated garnets (Figure 9c), show top-to-SSE shearing, indicating slip on an oblique normal fault with a right lateral strike-slip component (Figure 8).

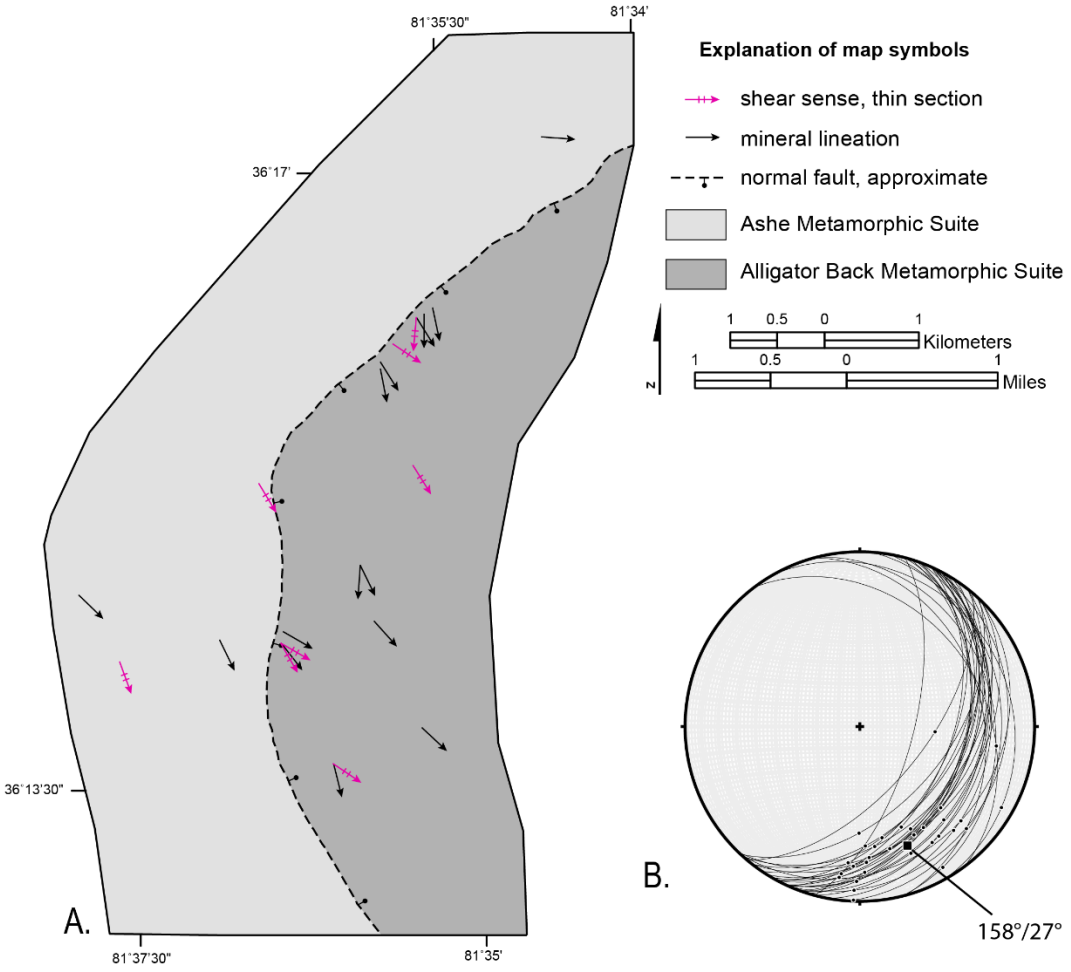

Figure 8: (A) Simplified map of contact between AMS and ABMS showing the orientations of mineral stretching lineations and shear sense determined in thin section. (B). Equal-area plot (lower hemisphere) of foliation planes and lineations measured in the field with an average mineral lineation trend of 158˚ and plunge 27˚.

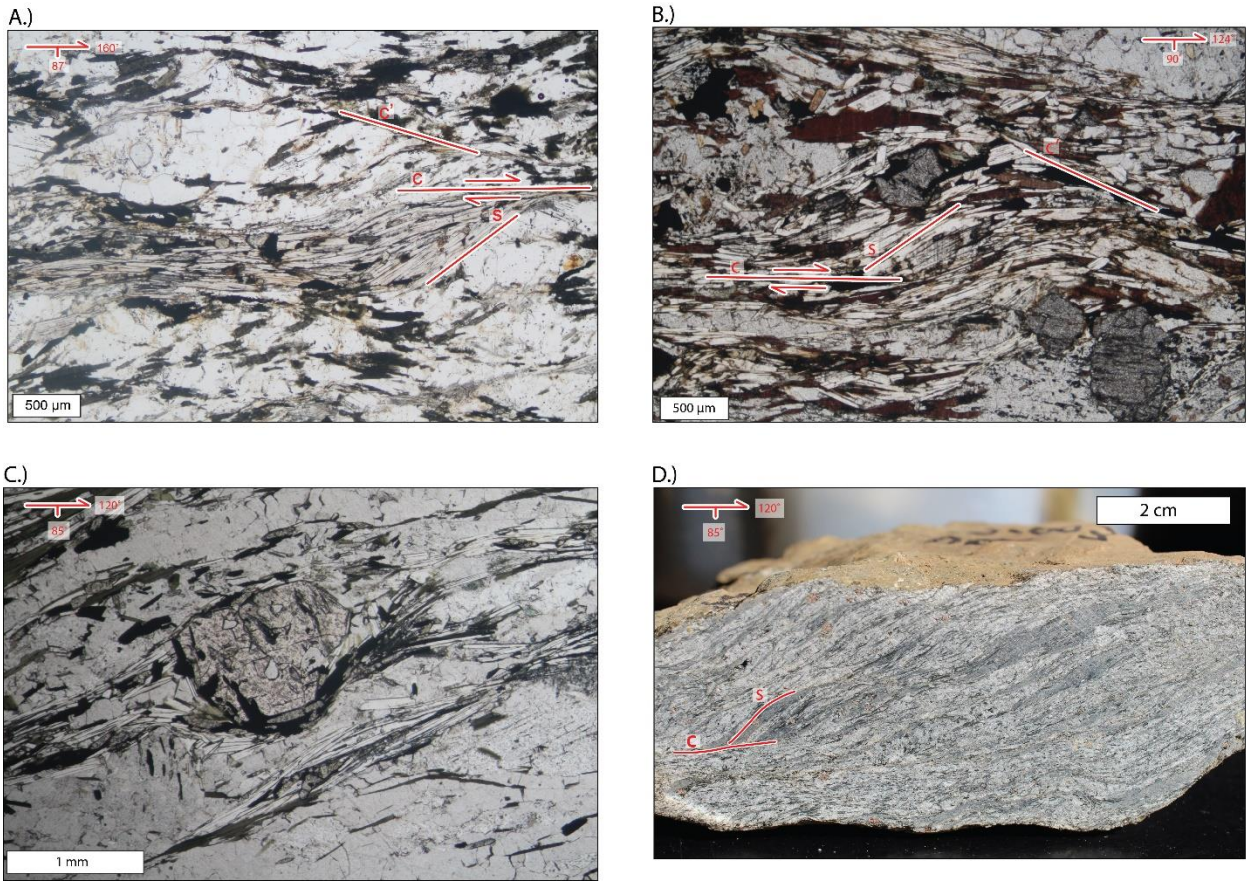

Figure 9: Photographs showing top to the SE shearing along the ductile normal fault. (A-B) Photomicrograph of S-C and C' fabric in thin section showing top-to-SE shearing (A: Zag, 36.236900˚N, 81.627277˚W; B: Zabg, 36.229011˚N, 81.598334˚W). (C) Photomicrograph of garnet showing top-to-SE rotation. (D) Photograph of hand sample cut along the vorticity profile plane. S-C fabric indicates top-to-SE shearing (C, D: Zabg, 36.239287˚N, 81.607970˚W).

Metamorphic conditions during shearing

The gneiss and schists within the Grassy Creek fault contain abundant quartz and feldspar, which allow for an estimation of temperatures associated with deformation (Simpson, 1985; Urai et al., 1986; Hirth and Tullis, 1992; Tullis, 2002; Stipp et al., 2002; Passchier and Trouw, 2005; Cisneroz-Lazaro et al., 2019). Deformation mechanisms include bulging recrystallization (BLG), subgrain-rotation recrystallization (SGR), and grain-boundary migration (GBM). BLG is characterized by irregular, blurry grain boundaries with very fine strain-free new grains. SGR is characterized by new grains and subgrains with similar sizes and elongated or

ribbon-shaped old grains with strong undulose extinction. GBM characteristics include varied grain size but generally coarser, nearly strain-free grains as well as lobate grain boundaries and pinning of grain boundary mobility structures (Simpson, 1985; Hirth and Tullis, 1992; Passchier and Trouw, 2005).

Quartz deformation has been studied experimentally and in naturally strained rocks (Hirth & Tullis, 1992; Simpson, 1985; Stipp et al., 2002; Tullis, 2002; Urai et al., 1986). At lower to middle greenschist facies (~300-400 C), quartz deforms dominantly by BLG. SGR is dominant at middle-to-upper greenschist facies (~400-500 C), but BLG may still occur at lower temperatures. At amphibolite facies (~500-700 C), quartz deforms dominantly by GBM. The deformation mechanisms of plagioclase and K-feldspar are similar and therefore treated together. Feldspar is stronger than quartz and encounters the recrystallization regimes experienced in quartz at higher temperatures (Cisneroz-Lazaro et al., 2019; Simpson, 1985; Tullis, 2002; Urai et al., 1986). BLG may occur at middle to upper greenschist facies (~400-500 C) but does not become dominant until lower-amphibolite facies (~450-600 C). SGR and BLG occur at amphibolite facies (600-700 C) along with abundant myrmekite.

Microstructures in quartz show dominant GBM and some evidence of SGR. The quartz grain boundaries are generally lobate and amoeboid in shape with a mostly recovered, strain-free appearance (Figure 10a, b). There is also abundant pinning of mica grains within the quartz (Figure 10c). Feldspar within the schist and gneiss show evidence of recrystallization dominantly by SGR. Synkinematic myrmekite is also abundant within the feldspar grains (Figure 10d). These deformation mechanisms indicate temperatures of around 500˚C to 600˚C, placing this deformation at amphibolite facies. Chlorite appears within the shear zone of the Grassy Creek

fault, which may indicate later greenschist facies reactivation of the Grassy Creek fault (Figures 11 and 12).

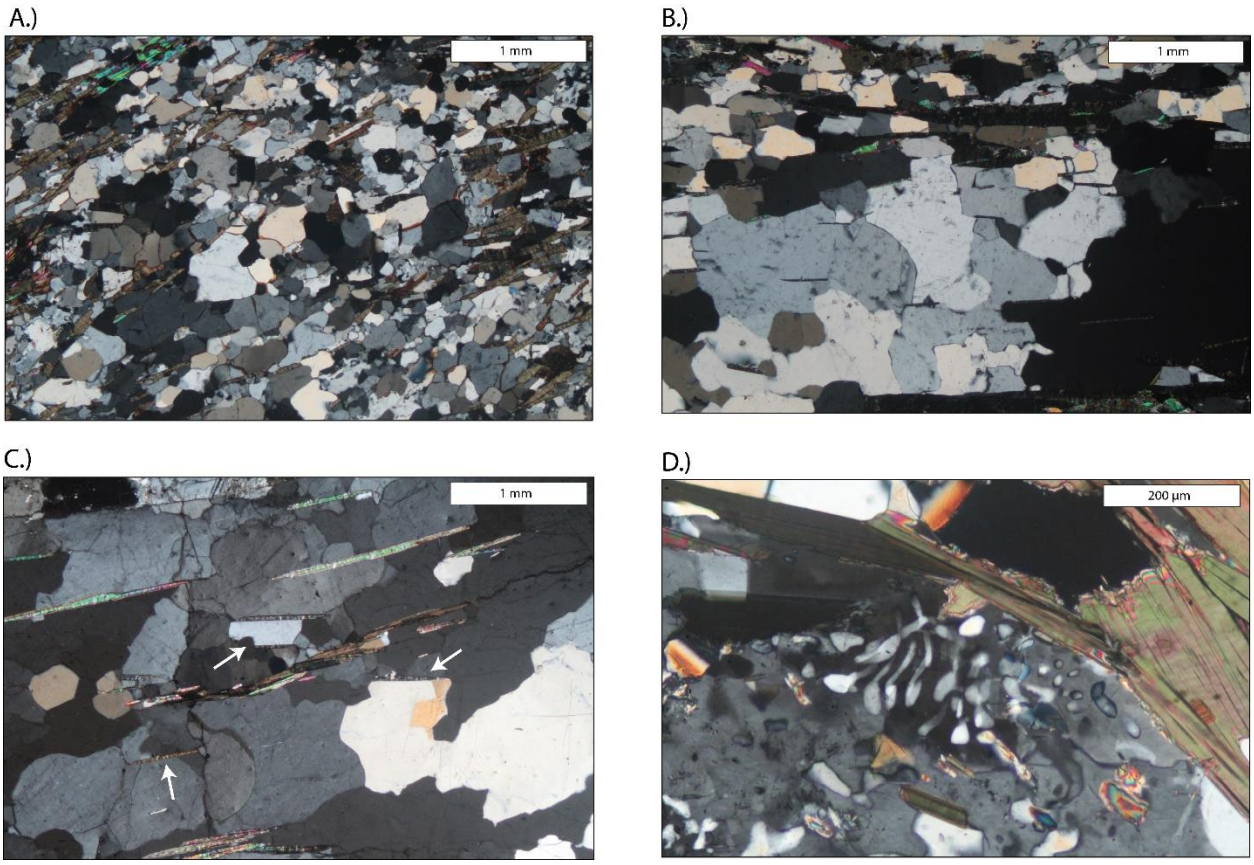

Figure 10: Photomicrographs (cross-polarized light) showing dynamic recrystallization in quartz and feldspar. (A) Quartz and feldspar grains showing dynamic recrystallization (Zabg, 36.263314˚N, 81.592795˚W). (B) Lobate, mostly strain free, quartz grains (Zabg, 36.268673˚N, 81.594709˚W). (C) Lobate quartz grains and arrows pointing to locations of mica pinning (Zabg, 36.239287˚N, 81.607970˚W). (D) Synkinematic myrmekite in feldspar grain (Zabg, 36.229011˚N, 81.598334˚W).

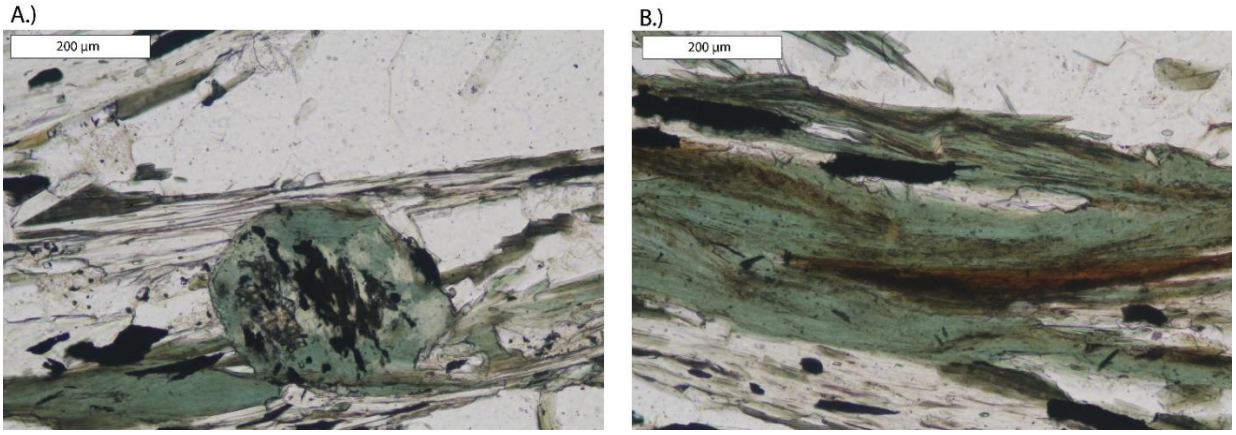

Figure 11: Photomicrographs (Plane light) showing chlorite replacing garnet (A) and biotite (B) within the shear zone of Grassy Creek fault (Zabg, 36.246219˚N, 81.542123˚W).

Change in metamorphic grade across the fault zone

Rocks within the EBR have experienced peak amphibolite-to-granulite facies of a regional Barrovian metamorphism during the Taconic orogeny (Thompson, 1957; Goldberg and Dallmeyer, 1997). Metamorphosed pelitic rocks within the AMS and the ABMS just north of the GMW include the index minerals chlorite, biotite, garnet, staurolite, kyanite, and sillimanite, in order of increasing metamorphic grade. We used the presence of these minerals to document changes in metamorphic grade across the map area and the Grassy Creek fault.

We identified biotite and garnet zones in the hanging wall of the Grassy Creek fault, indicating upper greenschist to lower amphibolite facies metamorphism. We identified garnet, kyanite, and sillimanite zones in the footwall of the fault, indicating upper amphibolite-to-granulite facies metamorphism (Figure 11). Staurolite coexists with kyanite in the eastern portion of the kyanite zone. The fault lies within the garnet zone and there does not appear to be a clear metamorphic break across the fault zone.

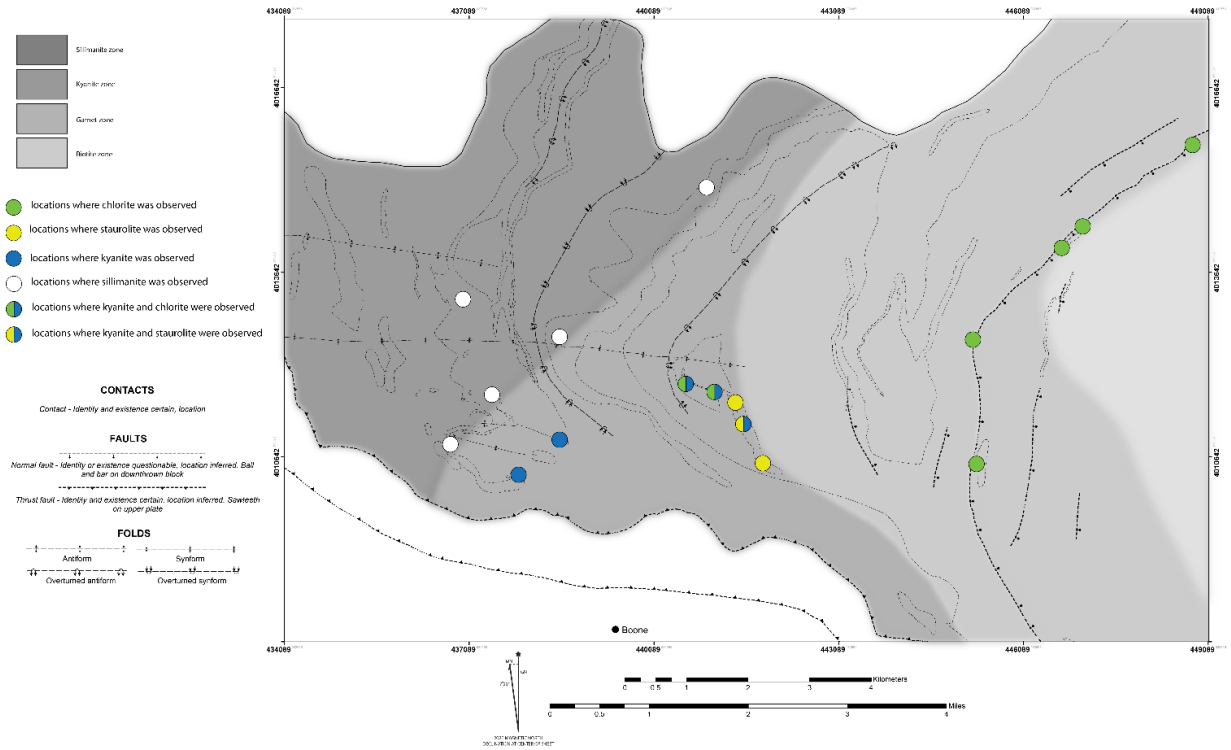

Figure 12: Sillimanite, kyanite, garnet, and biotite zones were drawn based on the locations of thin sections in which the listed index minerals were identified. Circles indicate the location of index minerals chlorite, staurolite, kyanite, and sillimanite.

Retrograded eclogite north of the GMW was first identified by Abbott and Greenwood (2001), distinguished from otherwise typical amphibolite by the amphibole + feldspar coronas surrounding the garnets. The retrograded eclogite consists of mineralogy and textures that indicate amphibolite facies retrogression of an original eclogite assemblage (Figure 13a). The amphibolite facies assemblage identified by Abbott and Greenwood (2001) is characterized by (diopside + plagioclase) + garnet + epidote + hornblende + quartz. Abbott and Greenwood (2001) found that the contacts between the retrograded eclogite and amphibolite are gradational and suggest that a significant volume of the amphibolite in the base of the AMS is retrograded eclogite.

We mapped other bodies of retrograded eclogite within the field area based on the distinct amphibolite + feldspar coronas around the garnets. Most of these locations are within ~4 km of the previously mapped retrograded eclogite, but one of the bodies is ~10 km SE from the others and 1.5 km west of the Grassy Creek fault (Figure 3). We identified the mineralogy of the retrograded eclogite that lies 1.5 km west of the Grassy Creek fault (Figure 13b) through thin section and Scanning Electron Microscope (SEM) analyses. This rock contains hornblende, plagioclase, quartz, garnet, epidote, and rutile. The mineral assemblage and textures suggest that this rock is in amphibolite facies retrogression with the mineral assemblage of plagioclase + garnet + epidote + hornblende + quartz.

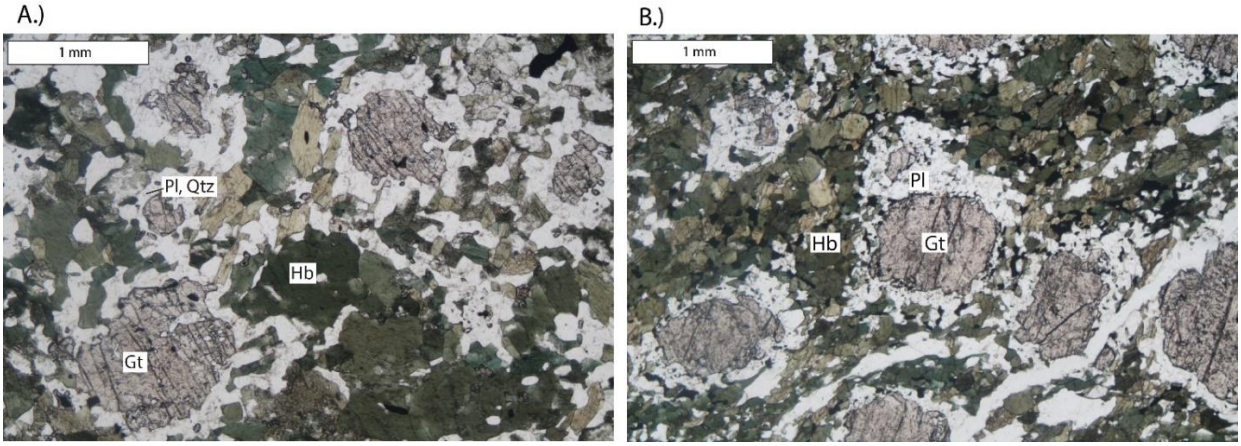

Figure 13: A.) Photomicrography (plane light) of retrograded eclogite previously mapped by Abbott and Greenwood (2001). Gt = garnet, Hb = hornblende, Pl = plagioclase, Qtz = quartz (36.249833˚N, 81.716003˚W). B.) Photomicrograph (plane light) of plagioclase feldspar (Pl) surrounding garnet (Gt). Hornblende (Hb) surrounds the feldspar 'halo' texture that was used to distinguish retrograded eclogite withing the field area. This sample was collected ~10 km SE of the originally mapped retrograded eclogite and in the footwall ~1.5 km west of the normal fault (36.218710˚N, 81.622055˚W).

Discussion

Lineaments

The dominant fractures throughout the field area, striking 98˚ and 113˚, are subparallel to the lineaments and the Boone fault. The less dominant NE-SW and NW-SE sets correspond with fractures found throughout the Blue Ridge and are likely associated with Alleghanian NW-directed shortening (Hibbard et al., 2006). Dominant fractures within L1 are subparallel to the lineaments, suggesting that this lineament is fracture controlled. Though L2 fractures show a dominant strike of 73˚, which may be due to the low sample size of 31 fractures, this lineament is parallel to L1, which suggests a similar origin and may also be a fracture zone. The parallel relationship between all of the lineaments within the field area suggests a similar origin. Therefore, each lineament has been interpreted to be a fracture zone based on the analysis of L1. The contact between gneiss and amphibolite crosses the L1 and L2 lineaments multiple times. We did not map measurable offset of the geologic contacts across the lineaments, which would indicate a fault. However, there may be a minor offset that was undetectable during our mapping.

The transition from the high topography to the lower topography corresponds to the boundary between a dominant rock type of amphibolite in the west and gneiss in the east. This change in lithology is likely responsible for the well-defined lineaments to the west due to the lower erodibility of the amphibolite compared to the gneiss. Because of this, erosion may be concentrated in fracture zones, creating well-developed lineaments in the West domain while erosion throughout the East domain is more widespread. The lithology may also explain the lack of lineament parallel fractures measured within the West domain due to the large number of fractures measured outside the lineaments. Smaller, less defined lineaments are also visible in the

eastern domain, where the dominant fractures measured are parallel to the lineaments and the Boone fault.

The paleostress analysis for brittle faults in set A yields a stress tensor with vertical maximum compression and NE-directed minimum compression. This stress tensor does not match the stresses that drove NW-directed Alleghanian shortening or Mesozoic E-W rifting but corresponds with NE-SW extension associated with Cenozoic uplift. Hill (2018) suggests the formation of the Boone fault was driven by Cenozoic uplift of the southern Appalachians. Set B yields a stress tensor with NW-directed maximum compression, corresponding with the Alleghanian NW-directed shortening. Though most of the lineament-parallel faults lie within set B, these faults and fractures may have formed during Alleghanian shortening and were later reactivated within the stress field associated with Cenozoic uplift. This is supported by the fact that the well-defined lineaments cut all Paleozoic structures and post-date the Alleghanian orogeny. Recent activity along two faults that correspond with lineaments within the southern Appalachians also supports the hypothesis that these lineaments formed during the recent uplift of the southern Appalachians (Hill, 2018, Hill et al., 2020a).

The Grassy Creek fault

The kinematic analyses of the Grassy Creek fault show top-to-SE normal faulting at amphibolite facies metamorphism. Lower-grade index minerals in the hanging wall and higher-grade index minerals in the footwall are consistent with normal motion along the fault. No clear break in metamorphic grade across the fault zone may indicate that the offset along the fault was not large enough to juxtapose two different metamorphic zones or an overprint of a lower grade metamorphic event that occurred after the dynamic metamorphism along the fault. Chlorite,

which appears to replace biotite and garnet within the shear zone, may suggest overprinting or reactivation during a later, greenschist-facies event.

The rocks within the southern Appalachians have experienced two episodes of rifting that may be responsible for the formation of an extensional fault. The rifting of Rodinia, ~565 Ma, occurred prior to the formation of the rocks within the Eastern Blue Ridge and cannot explain normal faulting along the Grassy Creek fault. The late Triassic rifting of Pangea produced brittle extensional structures that did not form during the same metamorphic conditions, amphibolite facies, experienced along the Grassy Creek fault. The Burnsville fault and the Gossan Lead fault are two Devonian-Mississippian, amphibolite facies strike-slip faults identified within the southern Appalachians (Trupe et al., 2003; Levine et al., 2018). At similar metamorphic conditions, the Grassy Creek fault is likely Devonian-Mississippian in age. The presence of chlorite within the shear zone may indicate later reactivation at greenschist facies, likely during the Paleozoic Alleghanian orogeny.

Synorogenic or pre-collisional extension may be responsible for the formation of the Grassy Creek fault. Synorogenic extension, resulting from underplating and overthickening of the crust, may have occurred during the Devonian-Mississippian Acadian-Neoacadian orogeny. Pre-collisional extension resulting from slab pull of the subducting plate may have occurred prior to the collisional events of the Acadian-Neoacadian orogeny. Both of these mechanisms could be responsible for the emplacement of high-pressure rocks, such as eclogite, over more recently accreted, lower-grade material. The presence of retrograded eclogite along the base of the AMS north of the GMW suggests that an eclogite facies terrane lies within the footwall of the Grassy

Creek fault and that the fault may have played a role in the exhumation of this eclogite facies terrane.

Conclusions

Despite the lack of an active plate boundary since the late Triassic, the Appalachians share many characteristics with tectonically active settings. A set of topographic lineaments parallel to the Boone fault are likely fracture zones that may have formed as a result of NE-extension due to Miocene doming of the southern Appalachians. These results may suggest that the origin of the lineaments within our field area is related to the event that formed the Boone fault and supports the hypotheses that the southern Appalachians have undergone Neogene uplift.

The southern Appalachians have recorded the complex history of multiple Wilson cycles that consists of deposition, magmatism, metamorphism, faulting, and overprinting. The formation of supercontinent Pangea and the Appalachian Mountain range consisted of three separate orogenies that began with the Ordovician Taconic orogeny ~460 Ma. Normal faulting along the Grassy Creek fault in the Eastern Blue Ridge of the southern Appalachians may have occurred as a result of synorogenic or pre-collision extension during the Devonian-Mississippian. The Grassy Creek fault is one of the first amphibolite facies normal faults identified within the southern Appalachians and may be responsible for the exhumation of the high-pressure eclogite facies terrane within the AMS. Further research into this fault will provide more information on the timing and magnitude of shearing as well as how normal faults have played a role in the formation of the southern Appalachians.

APPENDIX

Rock descriptions for 1:12,000 scale bedrock map

Ashe Metamorphic Suite

Amphibolite and garnet amphibolite (Zaa): dark green to black, fine-to-coarse grained, and appear weakly to strongly foliated. The mineralogy consists of hornblende, plagioclase feldspar, quartz, epidote, and garnet.

Gneiss (Zag): light tan to gray, fine-to-medium grained, and weakly-to-strongly foliated. AMS gneiss consists of quartz, plagioclase feldspar, biotite, muscovite, and garnet.

Retrograded eclogite (Zae): first recognized by Abbott and Greenwood (2001), dark green to black, medium-to-coarse grained, and weakly foliated. Mineralogy consists of hornblende, plagioclase feldspar, garnet, epidote, diopside, and rutile. Hornblende and feldspar occur as ‘halos’ around the garnets.

Staurolite-kyanite schist (Zass): medium brown to gray, medium grained to coarse grained, and strongly foliated to mylonitic. The mineralogy consists of muscovite, feldspar, garnet, quartz, biotite, and staurolite.

Hornblende gneiss (Zahg): medium-to-light gray, medium grained, and weakly to non-foliated. Mineralogy includes quartz, feldspar, hornblende, biotite, garnet, and chlorite.

Mica schist (Zams): medium gray to light gray, fine-to-medium grained, and foliated to mylonitic. Mica schist consists of muscovite, biotite, quartz, and feldspar.

Chlorite gneiss (Zacg): medium-to-light gray, medium grained, and weakly to non-foliated. The mineralogy consists of quartz, feldspar, biotite, chlorite, garnet, and titanite.

Pegmatite (Pzpg): white to light gray, coarse grained, and non-foliated. The mineralogy of the pegmatite consists of plagioclase feldspar, quartz, muscovite, and biotite.

Alligator Back Metamorphic Suite

Gneiss (Zabg): medium-to-light gray, fine-to-medium grained, and weakly foliated to mylonitic. ABMS gneiss consists of quartz, feldspar, biotite, muscovite, garnet, calcite, magnetite, and tourmaline.

Schist (Zabs): medium gray to light gray, medium-to-coarse grained, and strongly foliated to mylonitic. The mineralogy consists of muscovite, biotite, quartz, feldspar, garnet, chlorite, magnetite, and pyrite.

Amphibolite (Zaba): dark green to black, fine grained, and strongly foliated. ABMS amphibolite consists of hornblende, plagioclase feldspar, and quartz.

REFERENCES

Abbott, R. N., 1984, The greenschist–amphibolite transition in the CFM projection. American Mineralogist, v. 69(3-4), p. 250-251.

Abbott, R. N., & Greenwood, J. P., 2001, Retrograde metamorphism of eclogite in the southern Appalachian Mountains, USA–A case involving seamount subduction?. Journal of Metamorphic Geology, v. 19(4), p. 433-443.

Abbott, R. N., & Raymond, L. A., 1984, The Ashe metamorphic suite, northwest North Carolina; metamorphism and observations on geologic history. American Journal of Science, v. 284(4-5), p. 350-375.

Abbott, R. N., & Raymond, L. A., 1997, Petrology of pelitic and mafic rocks in the Ashe and Alligator Back Metamorphic Suites, northeast of the Grandfather Mountain window. Paleozoic Structure, Metamorphism, and Tectonics of the Blue Ridge of Western North Carolina, Carolina Geological Society, p. 87-100.

Adams, M. G., Stewart, K. G., Trupe, C. H. & Willard, R. A., 1995. Tectonic significance of high-pressure metamorphic rocks and dextral strike-slip faulting along the Taconic suture. In: Current Perspectives in the Appalachian-Caledonian Orogen (eds Hibbard, J.P., van Staal, C. R. & Cawood, P. A.). Geological Association Canada, pp. 21-42.

Adlakha, V., Patel, R. C., & Lal, N., 2013, Exhumation and its mechanisms: a review of exhumation studies in the Himalaya. Journal of the Geological Society of India, v. 81(4), p. 481-502.

Avigad, D., 1996, Pre-collisional ductile extension in the internal western Alps (Sesia zone, Italy). Earth and Planetary Science Letters, v. 137(1-4), p. 175-188.

Behrmann, J. H., 1988, Crustal-scale extension in a convergent orogen: the Sterzing-Steinach mylonite zone in the Eastern Alps. Geodinamica Acta, v. 2(2), p. 63-73.

Boyer, S. E., & Elliott, D., 1982, Thrust systems. The American Association of Petroleum Geologists Bulletin, v. 66(9), p. 1196-1230.

Bryant, B., & Reed Jr, J. C., 1970, Geology of the Grandfather Mountain window and vicinity, North Carolina and Tennessee, No. 615, US Govt. Print. Off.

Carter, M., & Merschat, A., 2014, Stratigraphy, structure, and regional correlation of eastern Blue Ridge sequences in southern Virginia and northwestern North Carolina: An interim report from new USGS mapping. In Elevating Geoscience in the Southeastern United States: New Ideas about Old Terranes: Field Guides for the GSA Southeastern Section Meeting, Blacksburg, Virginia, pp. 215-241.

Cattanach, B. L., Bozdog, G. N., Wooten, R. M., & Isard, S. J., 2016, A new bedrock geologic map of the southern half of the Montreat 7.5-minute quadrangle, Buncombe, McDowell, and Yancey counties, NC. Abstracts with Programs - Geological Society of America, 48(3), Abstract no. 27-5.

Cisneros-Lazaro, D. G., Miller, J. A., & Baumgartner, L. P., 2019, Role of myrmekite and associated deformation fabrics in controlling development of granitic mylonites in the Pofadder Shear Zone of southern Namibia. Contributions to Mineralogy and Petrology, v. 174(3), p. 1-20.

Dalmayrac, B., & Molnar, P., 1981, Parallel thrust and normal faulting in Peru and constraints on the state of stress. Earth and Planetary Science Letters, v. 55(3), p. 473-481.

Delvaux, D., & Sperner, B., 2003, New aspects of tectonic stress inversion with reference to the TENSOR program. Geological Society, London, Special Publications, v. 212(1), p. 75-100.

Dennison, J. M., and K. G. Stewart, 2001, Regional structural and stratigraphic evidence for dating Cenozoic uplift of Southern Appalachian highlands; Geological Society of America, Southeastern Section Meeting, Abstracts with Programs. Vol. 33. No. 6.

Dewey J.F., 1988, Extensional collapse of orogens. Tectonics 7, 1123–40.

England, P., & Houseman, G., 1989, Extension during continental convergence, with application to the Tibetan Plateau. Journal of Geophysical Research: Solid Earth, v. 94(B12), p. 17561-17579.

Galloway, W. E., Whiteaker, T. L., & Ganey-Curry, P., 2011, History of Cenozoic North American drainage basin evolution, sediment yield, and accumulation in the Gulf of Mexico basin. Geosphere, v. 7(4), p. 938-973.

Goldberg, S. A., & Dallmeyer, R. D., 1997, Chronology of Paleozoic metamorphism and deformation in the Blue Ridge thrust complex, North Carolina and Tennessee. American Journal of Science, v. 297(5), p. 488-526.

Gün, E., Pysklywec, R. N., Göğüş, O. H., & Topuz, G., 2021, Pre-collisional extension of microcontinental terranes by a subduction pulley. Nature Geoscience, v. 14(6), p. 443-450.

Hack, J. T., 1982, Physiographic divisions and differential uplift in the Piedmont and Blue Ridge: Geological Survey Professional Paper 1265, p. 49.

Hatcher, R. D.,2002, Alleghanian (Appalachian) orogeny, a product of zipper tectonics: Rotational transpressive continent-continent collision and closing of ancient oceans along irregular margins. Special Paper-Geological Society of America, v. 364, p. 199-208.

Hatcher, R. D., Bream, B. R., & Merschat, A. J., 2007, Tectonic map of the southern and central Appalachians: A tale of three orogens and a complete Wilson cycle. Geological Society of America Memoirs, v. 200, p. 595-632.

Hatcher Jr, R. D., Merschat, A. J., & Raymond, L. A., 2006, Geotraverse: Geology of northeastern Tennessee and the Grandfather Mountain region. In Geological Society of America 2006 Southeastern Section Meeting Field Trip Guidebook: Knoxville, University of Tennessee, pp. 129-184.

Hatcher, R. D. Jr., Merschat, A. J., & Thigpen, J. R., 2005, Blue ridge primer. Blue Ridge geotraverse east of the Great Smoky Mountains National Park, western North Carolina: Carolina Geological Society Guidebook, p. 1-24.

Hatcher, R. D., Tollo, R. P., Bartholomew, M. J., Hibbard, J. P., & Karabinos, P. M., 2010, The Appalachian orogen: A brief summary. From Rodinia to Pangea: The Lithotectonic Record of the Appalachian Region: Geological Society of America Memoir, 206, 1-19.

Hill, J. S., 2013, Zoned uplift of western North Carolina bounded by topographic lineaments, M.S. Thesis, University of North Carolina at Chapel Hill.

Hill, J. S., 2018, Post-Orogenic Uplift, Young Faults, and Mantle Reorganization in the Appalachians, Ph.D. Dissertation, The University of North Carolina at Chapel Hill.

Hill, J. S., Cattanach, B. L., Douglas, T. J., Figueiredo, P. M., Kirby, E., Korte, D. M., Lynn, A. S., Merschat, A. J., Owen, L. A., Scheip, C., Stewart, K. G., Wells, S. B., & Wooten, R. M. 2020a, Surface rupture of the Little River fault in response to the August 9, 2020 Mw 5.1 earthquake near Sparta, North Carolina. Poster Presentation at 2020 SCEC Annual Meeting.

Hill, J. S., Stewart, K. G., Figueiredo, P. M., Merschat, A., & Witt, A. V., 2020b, October, Current Understanding of Intraplate Seismicity and Surface Deformation Associated with the August 9th, 2020 Mw 5.1 Earthquake Near Sparta, North Carolina. In GSA 2020 Connects Online. GSA.

Hirth, G., & Tullis, J. A. N., 1992, Dislocation creep regimes in quartz aggregates. Journal of structural geology, v. 14(2), p. 145-159.

Levine, J. S. F., Merschat, A. J., McAleer, R. J., Casale, G., Quillan, K. R., Fraser, K. I., & BeDell, T. G., 2018, Kinematic, Deformational, and Thermochronologic Conditions Along the Gossan Lead and Fries Shear Zones: Constraining the Western-Eastern Blue Ridge Boundary in Northwestern North Carolina. Tectonics, v. 37(10), p. 3500-3523.

Malavieille, J., 2010, Impact of erosion, sedimentation, and structural heritage on the structure and kinematics of orogenic wedges: Analog models and case studies. GSA Today, v. 20(1), p. 4-10.

Miller, B. V., Fetter, A. H., & Stewart, K. G., 2006, Plutonism in three orogenic pulses, eastern Blue Ridge Province, southern Appalachians. Geological Society of America Bulletin, v. 118(1-2), p. 171-184.

Miller, B. V., Stewart, K. G., & Whitney, D. L., 2010, Three tectonothermal pulses recorded in eclogite and amphibolite of the Eastern Blue Ridge, Southern Appalachians. In From Rodinia to Pangea: The Lithotectonic Record of the Appalachian Region, pp. 701-724, Geological Society of America.

Misra, K. C., & Conte, J. A., 1991, Amphibolites of the Ashe and Alligator Back Formations, North Carolina: samples of late Proterozoic-early Paleozoic oceanic crust. Geological Society of America Bulletin, v. 103(6), p. 737-750.

Passchier, C. W., & Trouw, R. A., 2005, Microtectonics. Springer Science & Business Media.

Platt, J. P., 1986, Dynamics of orogenic wedges and the uplift of high-pressure metamorphic rocks. Geological society of America bulletin, 97(9), 1037-1053.

Poag, C. W., & Sevon, W. D., 1989, A record of Appalachian denudation in post-rift Mesozoic and Cenozoic sedimentary deposits of the US middle Atlantic continental margin. Geomorphology, v. 2(1-3), p. 119-157.

Rankin, D. W., 1969, The Fries fault: a major thrust in the Blue Ridge of southwestern Virginia. Geological Society of America Abstract with Programs, v. 4, No. 66.

Rankin, D. W., 1970, Stratigraphy and structure of Precambrian rocks in northwestern North Carolina: in Fisher, G. W. and others, eds., Studies of Appalachian Geology: Central and Southern: John Wiley and Sons, New York, p. 227-245.

Rankin, D. W., Espenshade. G.H., and Shaw, K. W., 1973, Stratigraphy and structure of the metamorphic belt in northwestern North Carolina and southwestern Virginia: A study from the Blue Ridge across the Brevard Fault Zone to the Sauratown Mountains Anticlinorium, American Journal of Science, p. 1-40.

Searle, M. P., & Lamont, T. N., 2020, Compressional metamorphic core complexes, low-angle normal faults and extensional fabrics in compressional tectonic settings. Geological Magazine, v. 157(1), p. 101-118.

Simpson, C., 1985, Deformation of granitic rocks across the brittle-ductile transition. Journal of structural geology, v. 7(5), p. 503-511.

Simpson, C., & Kalaghan, T., 1989, Late Precambrian crustal extension preserved in Fries fault zone mylonites, southern Appalachians. Geology, v. 17(2), p. 148-151.

Stewart, K. G., Dennison, J. M., 2006, Tertiary-to-recent arching and the age and origin of fracture-controlled lineaments in the southern Appalachians. Geological Society of America Abstracts with Programs, v. 38. No. 3.

Stewart, K. G., Hill, J. S., Wooten, R. M., Szymanski, E., Wells, S. B., Linking topographic lineaments in western North Carolina to active faults: Geological Society of America Abstracts with Programs, v. 52, No. 6.

Stipp, M., Stuenitz, H., Heilbronner, R., & Schmid, S. M., 2002, The eastern Tonale fault zone: a 'natural laboratory' for crystal plastic deformation of quartz over a temperature range from 250° to 700° C. Journal of Structural Geology, v. 24(12), p. 1861-1884.

Stose, A. J., & Stose, G. W., 1957, Geology and mineral resources of the Gossan Lead District and adjacent areas in Virginia. Virginia Division of Mineral Resources Bulletin, v. 72.

Thompson, Jr., J. B., 1957, The graphical analysis of mineral assemblages in pelitic schists. American Mineralogist: Journal of Earth and Planetary Materials, v. 42(11-12), p. 842-858.

Trupe, C. H., 1997, Deformation and metamorphism in part of the Blue Ridge thrust complex, northwestern North Carolina, Ph.D. Dissertation, The University of North Carolina at Chapel Hill.

Trupe, C. H., Butler, J. R., Mies, J. W., Adams, M. G., & Goldberg, S. A., 1990, The Linville Falls fault and related shear zone. In Geological Society of America Abstracts with Programs, v. 22, p. 66.

Trupe, C. H., Stewart, K. G., Adams, M. G., & Foudy, J. P., 2004, Deciphering the Grenville of the southern Appalachians through the post-Grenville tectonic history in northwestern North Carolina. Geological Society of America Memoirs, v. 197, p. 679-695.

Trupe, C. H., Stewart, K. G., Adams, M. G., Waters, C. L., Miller, B. V., & Hewitt, L. K., 2003, The Burnsville fault: Evidence for the timing and kinematics of southern Appalachian Acadian dextral transform tectonics. Geological Society of America Bulletin, v. 115, p. 1365-1376.

Tull, J. F., Allison, D. T., Whiting, S. E., & John, N. L., 2010, Southern Appalachian Laurentian margin initial drift-facies sequences: implications for margin evolution. Geological Society of America Memoirs, v. 206, p. 935-956.

Tullis, J., 2002, Deformation of granitic rocks: Experimental studies and natural examples. Reviews in Mineralogy and Geochemistry, v. 51, p. 51-95.

Urai, J. L., Means, W. D., & Lister, G. S., 1986, Dynamic recrystallization of minerals. In Mineral and rock deformation: laboratory studies, v. 36, pp. 161-199 Washington, DC: AGU.

Willard, R. A., & Adams, M. G., 1994, Newly discovered eclogite in the southern Appalachian orogen, northwestern North Carolina. Earth and Planetary Science Letters, v. 123(1-3), p. 61-70.